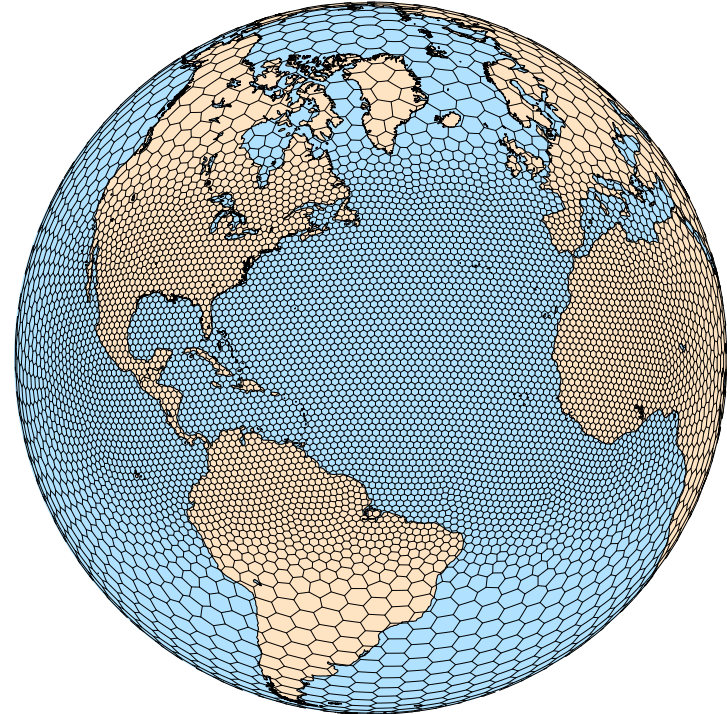


- Overview
- Mesh description
- *Atmospheric solver, physics*
- Registry, installation, running MPAS
- MPAS support, future evolution

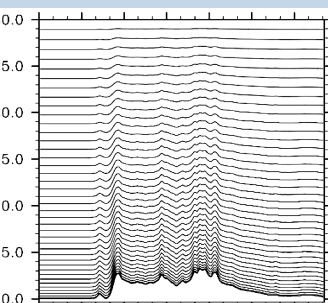
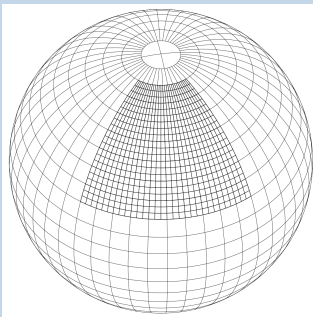
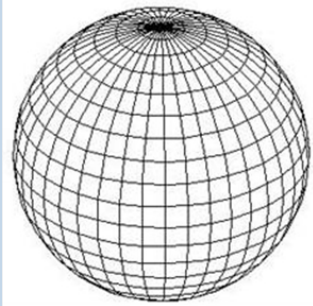


- Overview
- Mesh description
- *Atmospheric solver, physics*

*Vertical coordinate, horizontal discretization:
gradients, flux divergence, Coriolis term.
Configuration of dynamics and physics*

MPAS-Atmosphere solver

WRF Characteristics

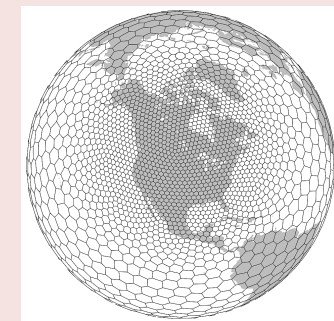
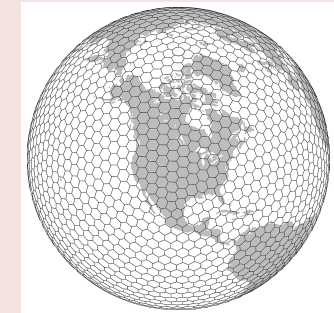


- Lat-Lon global grid
 - Anisotropic grid cells
 - Polar filtering required
 - Poor scaling on massively parallel computers

- Grid refinement through domain nesting
 - Flow distortions at nest boundaries

- Pressure-based terrain-following sigma vertical coordinate

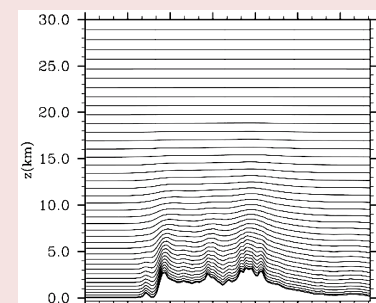
MPAS Characteristics



- Unstructured Voronoi (hexagonal) grid
 - Good scaling on massively parallel computers
 - No pole problems

- Smooth grid refinement on a conformal mesh
 - Increased accuracy and flexibility in varying resolution

- Height-based hybrid smoothed terrain-following vertical coordinate
 - Improved numerical accuracy

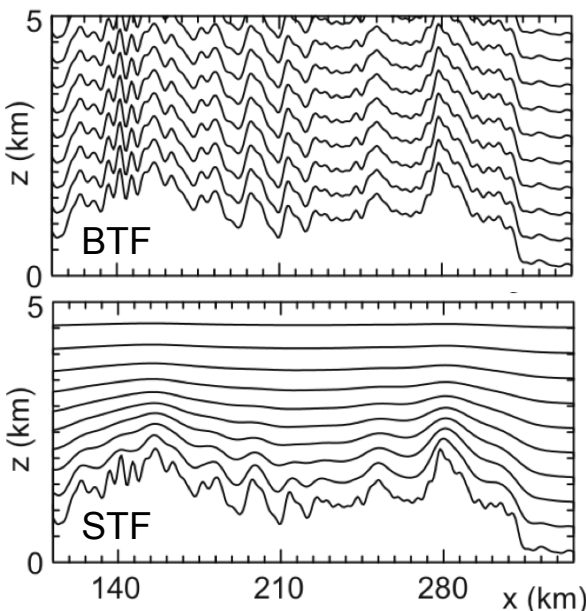


MPAS Vertical Mesh

Specification of terrain:

- High resolution terrain data (30 arcsec) averaged over grid-cell area
- Terrain smoothing with one pass of a 4th order Laplacian

Smoothed Terrain-Following (STF) hybrid Coordinate



$$z(x, y, \zeta) = \zeta + A(\zeta)h_s(x, y, \zeta)$$

$A(\zeta)$ Controls rate at which terrain influences are attenuated with height

$h_s(x, y, \zeta)$ Terrain influence that represents increased smoothing of the actual terrain with height

Multiple passes of simple Laplacian smoother at each ζ level:

$$h_s^{(n)} = h_s^{(n-1)} + \beta(\zeta)d^2 \nabla_\zeta^2 h_s^{(n-1)}$$

STF progressively smooths coordinate surfaces while transitioning to a height coordinate

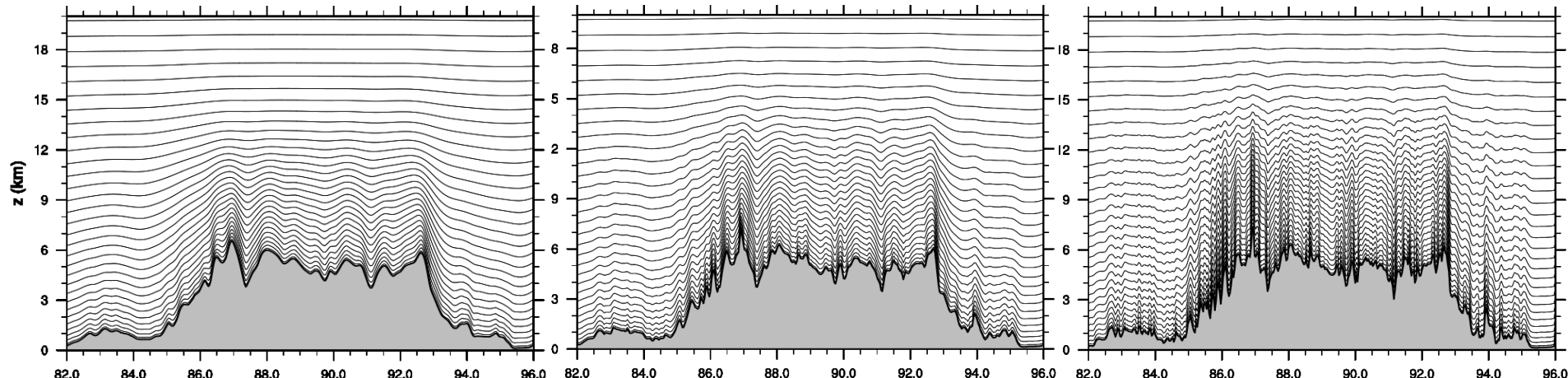
15, 7.5, & 3 km MPAS - Tibetan Plateau, 28° N

15 km grid

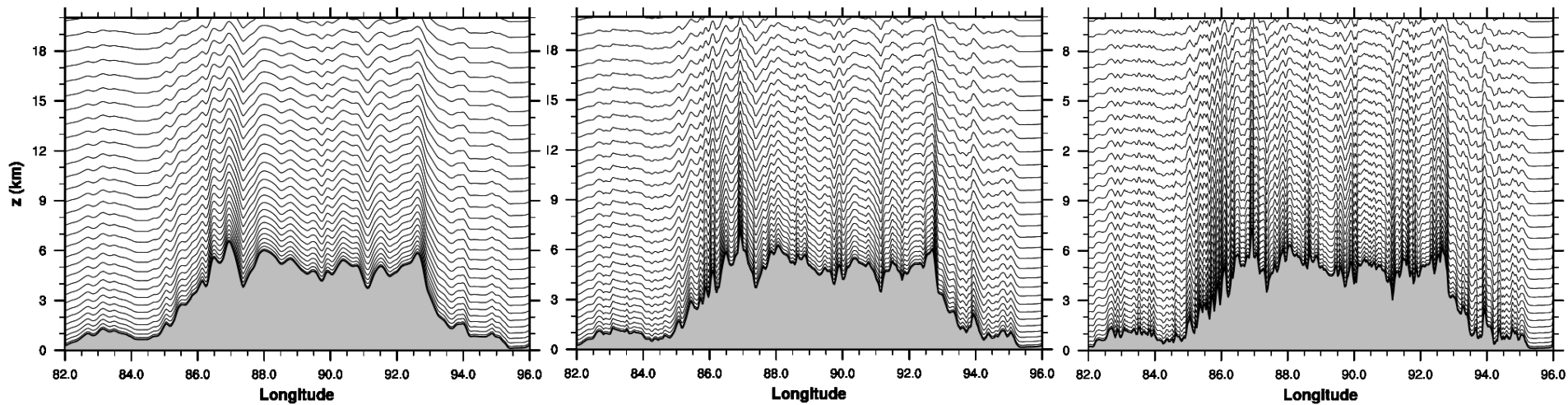
7.5 km grid

3 km grid

Smoothed hybrid terrain-following (STF) coordinate



Basic terrain-following (BTF) coordinate



(Model top is at 30 km)

MPAS Nonhydrostatic Atmospheric Solver

Nonhydrostatic formulation

Equations

- Prognostic equations for coupled variables.
- Generalized height coordinate.
- Horizontally vector invariant eqn set.
- Continuity equation for dry air mass.
- Thermodynamic equation for coupled potential temperature.

Time integration scheme

As in Advanced Research WRF -
Split-explicit Runge-Kutta (3rd order)

Variables:
 $(U, V, \Omega, \Theta, Q_j) = \tilde{\rho}_d \cdot (u, v, \dot{\eta}, \theta, q_j)$

Vertical coordinate:
 $z = \zeta + A(\zeta) h_s(x, y, \zeta)$

Prognostic equations:

$$\frac{\partial \mathbf{V}_H}{\partial t} = -\frac{\rho_d}{\rho_m} \left[\nabla_\zeta \left(\frac{p}{\zeta_z} \right) - \frac{\partial z_H p}{\partial \zeta} \right] - \eta \mathbf{k} \times \mathbf{V}_H \\ - \mathbf{v}_H \nabla_\zeta \cdot \mathbf{V} - \frac{\partial \Omega \mathbf{v}_H}{\partial \zeta} - \rho_d \nabla_\zeta K - eW \cos \alpha_r - \frac{uW}{r_e} + \mathbf{F}_{V_H},$$

$$\frac{\partial W}{\partial t} = -\frac{\rho_d}{\rho_m} \left[\frac{\partial p}{\partial \zeta} + g \tilde{\rho}_m \right] - (\nabla \cdot \mathbf{v} W)_\zeta \\ + \frac{uU + vV}{r_e} + e(U \cos \alpha_r - V \sin \alpha_r) + F_W,$$

$$\frac{\partial \Theta_m}{\partial t} = -(\nabla \cdot \mathbf{V} \theta_m)_\zeta + F_{\Theta_m},$$

$$\frac{\partial \tilde{\rho}_d}{\partial t} = -(\nabla \cdot \mathbf{V})_\zeta,$$

$$\frac{\partial Q_j}{\partial t} = -(\nabla \cdot \mathbf{V} q_j)_\zeta + \rho_d S_j + F_{Q_j},$$

Diagnostics and definitions:

$$\theta_m = \theta [1 + (R_v/R_d) q_v] \quad p = p_0 \left(\frac{R_d \zeta_z \Theta_m}{p_0} \right)^\gamma$$

$$\frac{\rho_m}{\rho_d} = 1 + q_v + q_c + q_r + \dots$$

MPAS Nonhydrostatic Atmospheric Solver

Prognostic
equations:

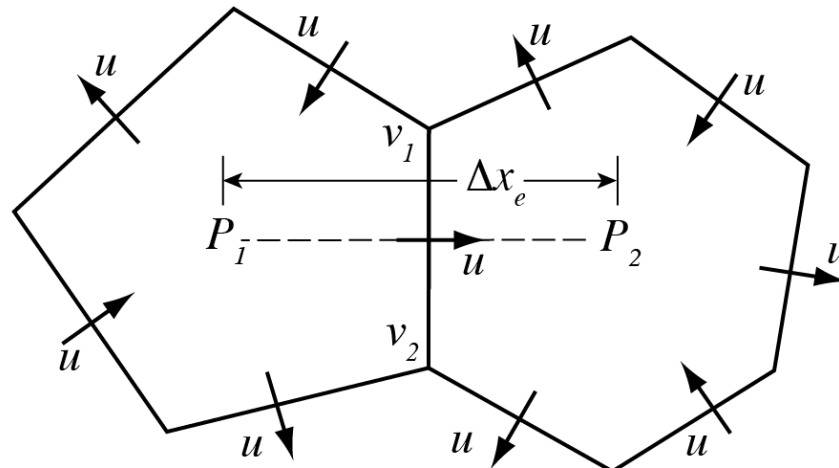
$$\begin{aligned}
 \frac{\partial \mathbf{V}_H}{\partial t} = & -\frac{\rho_d}{\rho_m} \left[\nabla_\zeta \left(\frac{p}{\zeta_z} \right) - \frac{\partial z_H p}{\partial \zeta} \right] - \eta \mathbf{k} \times \mathbf{V}_H \\
 & - \mathbf{v}_H \nabla_\zeta \cdot \mathbf{V} - \frac{\partial \Omega \mathbf{v}_H}{\partial \zeta} - \rho_d \nabla_\zeta K - eW \cos \alpha_r - \frac{uW}{r_e} + \mathbf{F}_{V_H}, \\
 \frac{\partial W}{\partial t} = & -\frac{\rho_d}{\rho_m} \left[\frac{\partial p}{\partial \zeta} + g \tilde{\rho}_m \right] - (\nabla \cdot \mathbf{v} W)_\zeta \\
 & + \frac{uU + vV}{r_e} + e(U \cos \alpha_r - V \sin \alpha_r) + F_W, \\
 \frac{\partial \Theta_m}{\partial t} = & -(\nabla \cdot \mathbf{V} \theta_m)_\zeta + F_{\Theta_m}, \\
 \frac{\partial \tilde{\rho}_d}{\partial t} = & -(\nabla \cdot \mathbf{V})_\zeta, \\
 \frac{\partial Q_j}{\partial t} = & -(\nabla \cdot \mathbf{V} q_j)_\zeta + \rho_d S_j + F_{Q_j},
 \end{aligned}$$

- (1) Gradient operators
- (2) Flux divergence operators
- (3) Nonlinear Coriolis term

Operators on the Voronoi Mesh

Pressure and KE gradients

$$\begin{aligned} \frac{\partial \mathbf{V}_H}{\partial t} = & -\frac{\rho_d}{\rho_m} \left[\nabla_\zeta \left(\frac{p}{\zeta_z} \right) - \frac{\partial z_H p}{\partial \zeta} \right] - \eta \mathbf{k} \times \mathbf{V}_H \\ & - \mathbf{v}_H \nabla_\zeta \cdot \mathbf{V} - \frac{\partial \Omega \mathbf{v}_H}{\partial \zeta} - \rho_d \nabla_\zeta K - eW \cos \alpha_r - \frac{uW}{r_e} + \mathbf{F}_{V_H}, \end{aligned}$$



On the Voronoi mesh, P_1P_2 is perpendicular to v_1v_2 and is bisected by v_1v_2 , hence $P_x \sim (P_2 - P_1)\Delta x_e^{-1}$ is 2nd order accurate.

Operators on the Voronoi Mesh

Flux divergence and transport

Transport equation, conservative form:

$$\frac{\partial(\rho\psi)}{\partial t} = -\nabla \cdot \mathbf{V}(\rho\psi)$$

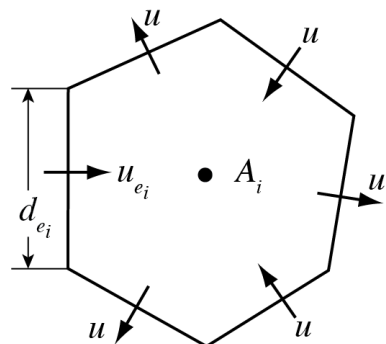
Finite-Volume formulation,
Integrate over cell:

$$\int_D \left[\frac{\partial}{\partial t}(\rho\psi) = -\nabla \cdot \mathbf{V}(\rho\psi) \right] dV$$

Apply divergence theorem:

$$\frac{\partial(\overline{\rho\psi})}{\partial t} = -\frac{1}{V} \int_{\Sigma} (\rho\psi) \mathbf{V} \cdot \mathbf{n} d\sigma$$

Discretize in time and space: $(\rho\psi)_i^{t+\Delta t} = (\rho\psi)_i^t - \Delta t \frac{1}{A_i} \sum_{n_{e_i}} d_{e_i} \overline{(\rho \mathbf{V} \cdot \mathbf{n}_{e_i}) \psi}$



Velocity divergence operator is 2nd-order accurate for edge-centered velocities.

Operators on the Voronoi Mesh

Flux divergence and transport

MPAS uses a Runge-Kutta time-integration scheme.

$$\frac{\partial(\rho\psi)}{\partial t} = L(\mathbf{V}, \rho, \psi)$$

$$(\rho\psi)^* = (\rho\psi)^t + \frac{\Delta t}{3} L(\mathbf{V}, \rho, \psi^t)$$

$$(\rho\psi)^{**} = (\rho\psi)^t + \frac{\Delta t}{2} L(\mathbf{V}, \rho, \psi^*)$$

$$(\rho\psi)^{t+\Delta t} = (\rho\psi)^t + \Delta t L(\mathbf{V}, \rho, \psi^{**})$$

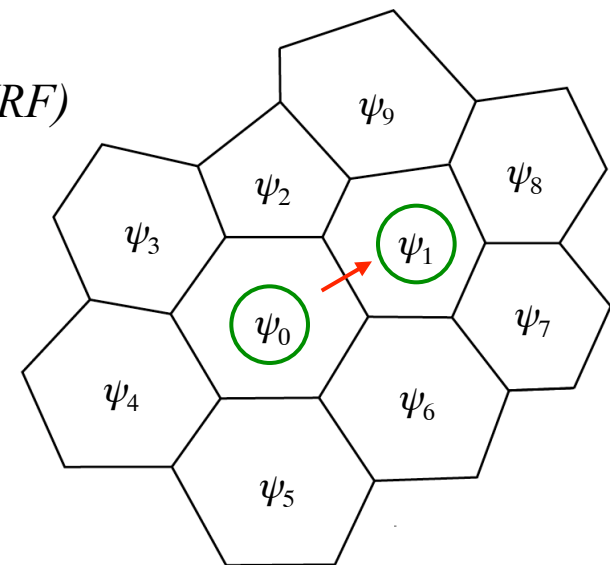
$$(\rho\psi)_i^{t+\Delta t} = (\rho\psi)_i^t - \Delta t \frac{1}{A_i} \sum_{n_{e_i}} d_{e_i} (\rho \mathbf{V} \cdot \mathbf{n}_{e_i}) \psi$$

Instantaneous
flux divergence in
RK-based scheme

Computing the flux - consider 1D transport (e.g. from WRF)

$$\frac{\partial(u\psi_i)}{\partial x} = \frac{1}{\Delta x} [F_{i+1/2}(u\psi) - F_{i-1/2}(u\psi)] + O(\Delta x^p).$$

2nd-order
flux: $F(u, \psi)_{i+1/2} = u_{i+1/2} \left[\frac{1}{2} (\psi_{i+1} + \psi_i) \right]$



Operators on the Voronoi Mesh

Flux divergence and transport

3rd and 4th-order fluxes:

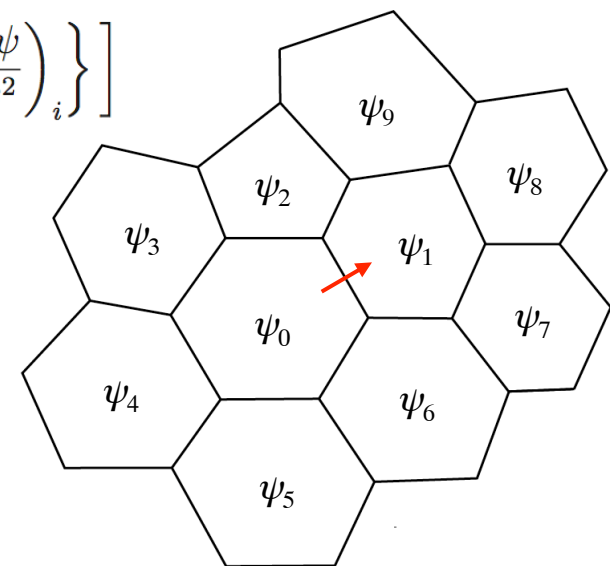
$$F(u, \psi)_{i+1/2} = u_{i+1/2} \left[\frac{1}{2} (\psi_{i+1} + \psi_i) - \frac{1}{12} (\delta_x^2 \psi_{i+1} + \delta_x^2 \psi_i) + \text{sign}(u) \frac{\beta}{12} (\delta_x^2 \psi_{i+1} - \delta_x^2 \psi_i) \right]$$

where $\delta_x^2 \psi_i = \psi_{i-1} - 2\psi_i + \psi_{i+1}$ (Hundsdorfer et al, 1995; Van Leer, 1985)

Recognizing $\delta_x^2 \psi = \Delta x^2 \frac{\partial^2 \psi}{\partial x^2} + O(\Delta x^4)$ we recast the 3rd and 4th order flux as

$$\begin{aligned} F(u, \psi)_{i+1/2} = u_{i+1/2} & \left[\frac{1}{2} (\psi_{i+1} + \psi_i) - \Delta x_e^2 \frac{1}{12} \left\{ \left(\frac{\partial^2 \psi}{\partial x^2} \right)_{i+1} + \left(\frac{\partial^2 \psi}{\partial x^2} \right)_i \right\} \right. \\ & \left. + \text{sign}(u) \Delta x_e^2 \frac{\beta}{12} \left\{ \left(\frac{\partial^2 \psi}{\partial x^2} \right)_{i+1} - \left(\frac{\partial^2 \psi}{\partial x^2} \right)_i \right\} \right] \end{aligned}$$

where x is the direction normal to the cell edge and i and $i+1$ are cell centers. We use the least-squares-fit polynomial to compute the second derivatives.



Operators on the Voronoi Mesh

Flux divergence and transport

3rd and 4th-order fluxes:

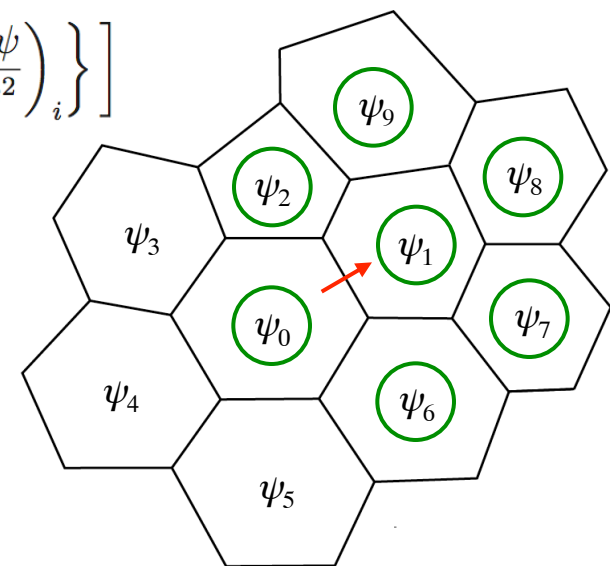
$$F(u, \psi)_{i+1/2} = u_{i+1/2} \left[\frac{1}{2} (\psi_{i+1} + \psi_i) - \frac{1}{12} (\delta_x^2 \psi_{i+1} + \delta_x^2 \psi_i) + \text{sign}(u) \frac{\beta}{12} (\delta_x^2 \psi_{i+1} - \delta_x^2 \psi_i) \right]$$

where $\delta_x^2 \psi_i = \psi_{i-1} - 2\psi_i + \psi_{i+1}$ (Hundsdorfer et al, 1995; Van Leer, 1985)

Recognizing $\delta_x^2 \psi = \Delta x^2 \frac{\partial^2 \psi}{\partial x^2} + O(\Delta x^4)$ we recast the 3rd and 4th order flux as

$$\begin{aligned} F(u, \psi)_{i+1/2} = u_{i+1/2} & \left[\frac{1}{2} (\psi_{i+1} + \psi_i) - \Delta x_e^2 \frac{1}{12} \left\{ \left(\frac{\partial^2 \psi}{\partial x^2} \right)_{i+1} + \left(\frac{\partial^2 \psi}{\partial x^2} \right)_i \right\} \right. \\ & \left. + \text{sign}(u) \Delta x_e^2 \frac{\beta}{12} \left\{ \left(\frac{\partial^2 \psi}{\partial x^2} \right)_{i+1} - \left(\frac{\partial^2 \psi}{\partial x^2} \right)_i \right\} \right] \end{aligned}$$

where x is the direction normal to the cell edge and i and $i+1$ are cell centers. We use the least-squares-fit polynomial to compute the second derivatives.



Operators on the Voronoi Mesh

Flux divergence and transport

3rd and 4th-order fluxes:

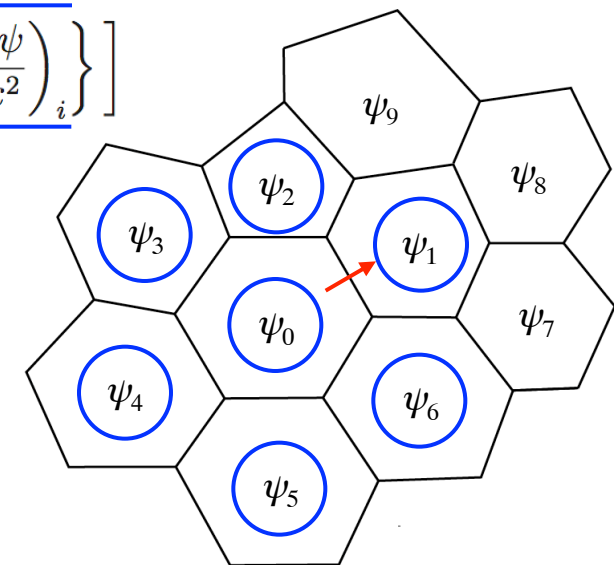
$$F(u, \psi)_{i+1/2} = u_{i+1/2} \left[\frac{1}{2} (\psi_{i+1} + \psi_i) - \frac{1}{12} (\delta_x^2 \psi_{i+1} + \delta_x^2 \psi_i) + \text{sign}(u) \frac{\beta}{12} (\delta_x^2 \psi_{i+1} - \delta_x^2 \psi_i) \right]$$

where $\delta_x^2 \psi_i = \psi_{i-1} - 2\psi_i + \psi_{i+1}$ (Hundsdorfer et al, 1995; Van Leer, 1985)

Recognizing $\delta_x^2 \psi = \Delta x^2 \frac{\partial^2 \psi}{\partial x^2} + O(\Delta x^4)$ we recast the 3rd and 4th order flux as

$$\begin{aligned} F(u, \psi)_{i+1/2} = u_{i+1/2} & \left[\frac{1}{2} (\psi_{i+1} + \psi_i) - \Delta x_e^2 \frac{1}{12} \left\{ \left(\frac{\partial^2 \psi}{\partial x^2} \right)_{i+1} + \left(\frac{\partial^2 \psi}{\partial x^2} \right)_i \right\} \right. \\ & \left. + \text{sign}(u) \Delta x_e^2 \frac{\beta}{12} \left\{ \left(\frac{\partial^2 \psi}{\partial x^2} \right)_{i+1} - \left(\frac{\partial^2 \psi}{\partial x^2} \right)_i \right\} \right] \end{aligned}$$

where x is the direction normal to the cell edge and i and $i+1$ are cell centers. We use the least-squares-fit polynomial to compute the second derivatives.



Operators on the Voronoi Mesh

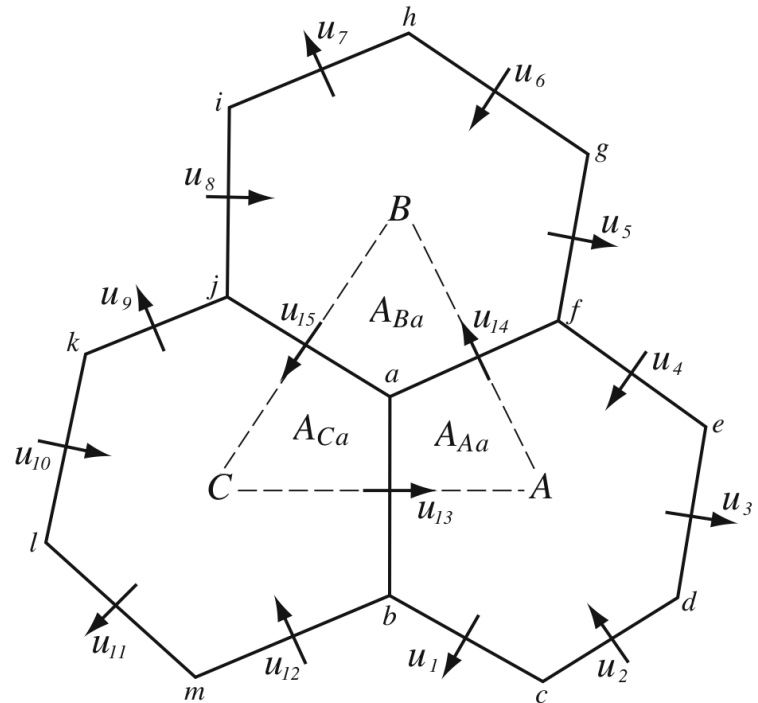
'Nonlinear' Coriolis force

$$\begin{aligned} \frac{\partial \mathbf{V}_H}{\partial t} = & -\frac{\rho_d}{\rho_m} \left[\nabla_\zeta \left(\frac{p}{\zeta_z} \right) - \frac{\partial \mathbf{z}_H p}{\partial \zeta} \right] - \eta \mathbf{k} \times \mathbf{V}_H \\ & - \mathbf{v}_H \nabla_\zeta \cdot \mathbf{V} - \frac{\partial \Omega \mathbf{v}_H}{\partial \zeta} - \rho_d \nabla_\zeta K - eW \cos \alpha_r - \frac{uW}{r_e} + \mathbf{F}_{V_H}, \end{aligned}$$

Vorticity is computed by evaluating the circulation around the triangles.

Vorticity *lives* on the vertices.

First, the linear piece: $\int \mathbf{k} \times \mathbf{V}_H$



Operators on the Voronoi Mesh 'Nonlinear' Coriolis force

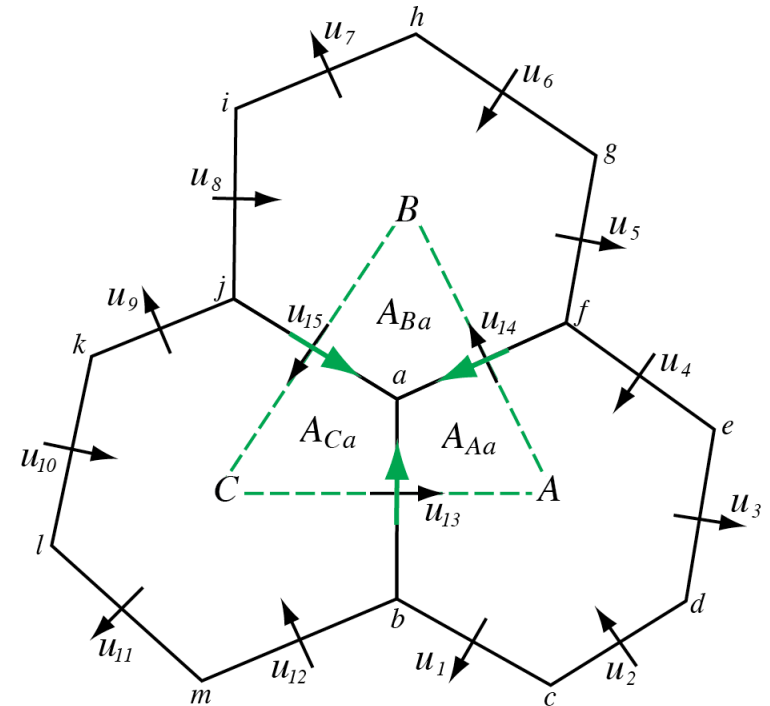
$$\begin{aligned} \frac{\partial \mathbf{V}_H}{\partial t} = & -\frac{\rho_d}{\rho_m} \left[\nabla_\zeta \left(\frac{p}{\zeta_z} \right) - \frac{\partial \mathbf{z}_H p}{\partial \zeta} \right] - \eta \mathbf{k} \times \mathbf{V}_H \\ & - \mathbf{v}_H \nabla_\zeta \cdot \mathbf{V} - \frac{\partial \Omega \mathbf{v}_H}{\partial \zeta} - \rho_d \nabla_\zeta K - eW \cos \alpha_r - \frac{uW}{r_e} + \mathbf{F}_{V_H}, \end{aligned}$$

Vorticity is computed by evaluating the circulation around the triangles.

Vorticity *lives* on the vertices.

First, the linear piece: $\int \mathbf{k} \times \mathbf{V}_H$

How do we compute the tangential velocity on the cell faces needed in the Coriolis term?



Operators on the Voronoi Mesh 'Nonlinear' Coriolis force

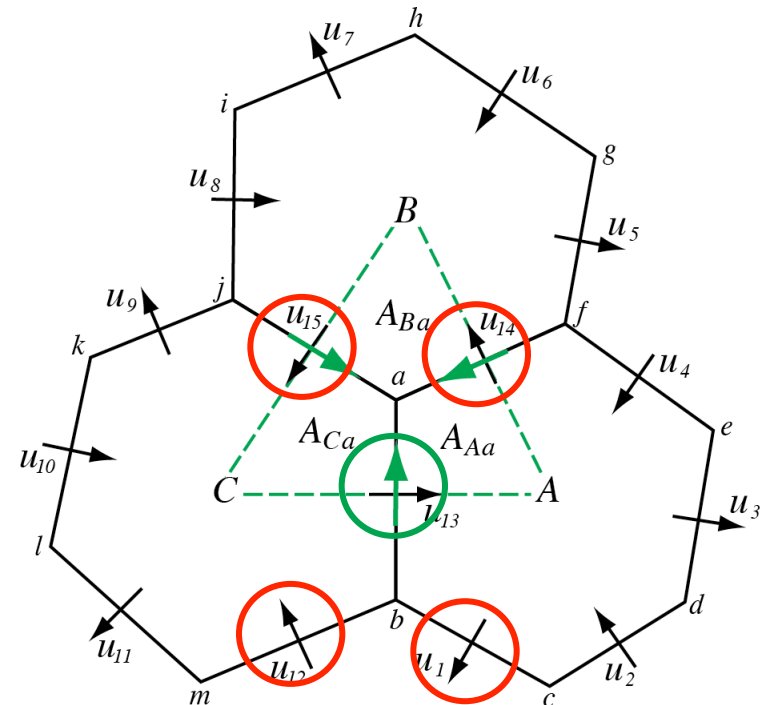
$$\begin{aligned} \frac{\partial \mathbf{V}_H}{\partial t} = & -\frac{\rho_d}{\rho_m} \left[\nabla_\zeta \left(\frac{p}{\zeta_z} \right) - \frac{\partial \mathbf{z}_H p}{\partial \zeta} \right] - \eta \mathbf{k} \times \mathbf{V}_H \\ & - \mathbf{v}_H \nabla_\zeta \cdot \mathbf{V} - \frac{\partial \Omega \mathbf{v}_H}{\partial \zeta} - \rho_d \nabla_\zeta K - eW \cos \alpha_r - \frac{uW}{r_e} + \mathbf{F}_{V_H}, \end{aligned}$$

Linear piece: $f \mathbf{k} \times \mathbf{V}_H$

Simplest approach: Construct tangential velocities from weighted sum of the four nearest neighbors.

Result: physically stationary geostrophic modes (geostrophically-balanced flow) will not be stationary in the discrete system; the solver is unusable.

(Nickovic et al, MWR 2002)



Operators on the Voronoi Mesh

'Nonlinear' Coriolis force

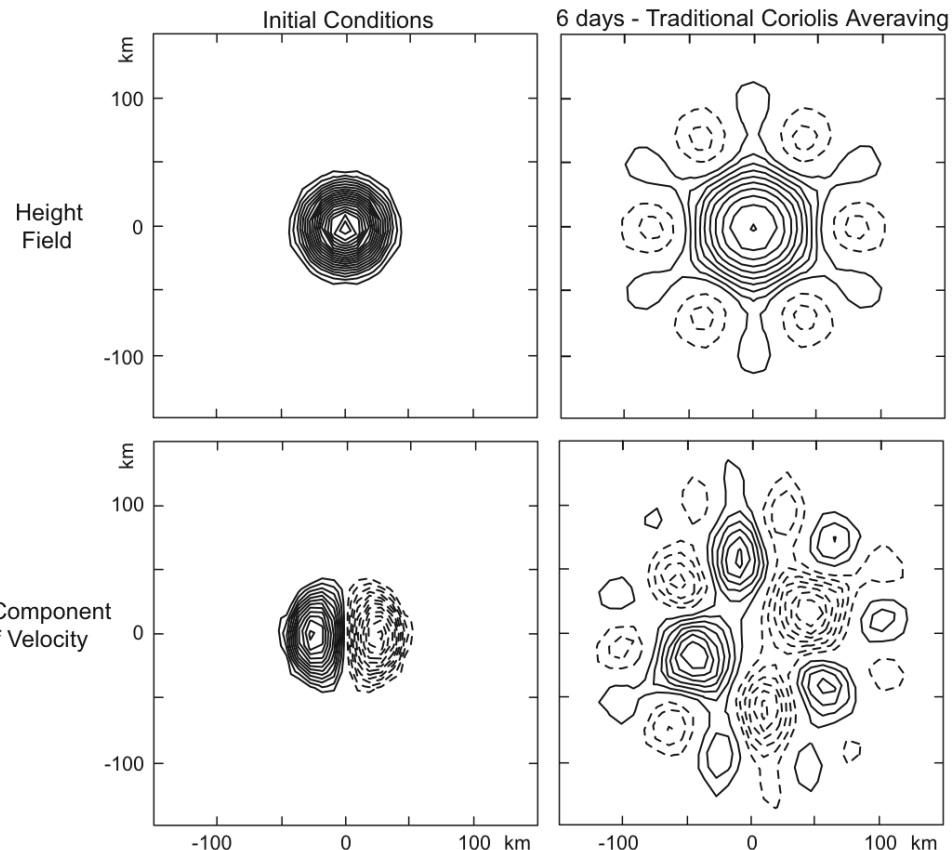
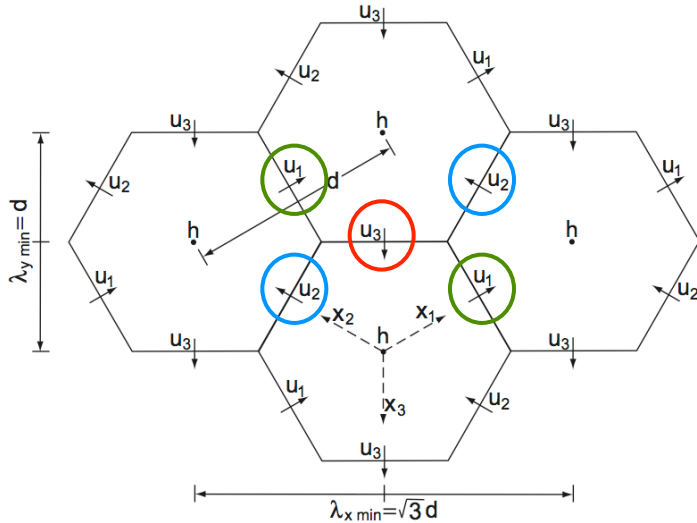
Linear piece: $f \ k \ x \ V_H$

$$\partial_t u_1 + g\delta_{x_1} h + \frac{f}{\sqrt{3}}(u_{31} - u_{21}) = 0$$

$$\partial_t u_2 + g\delta_{x_2} h + \frac{f}{\sqrt{3}}(u_{12} - u_{32}) = 0$$

$$\partial_t u_3 + g\delta_{x_3} h + \frac{f}{\sqrt{3}}(u_{23} + u_{13}) = 0$$

$$\partial_t h + \frac{2}{3}H(\delta_{x_1} u_1 + \delta_{x_2} u_2 + \delta_{x_3} u_3) = 0$$



Operators on the Voronoi Mesh

'Nonlinear' Coriolis force

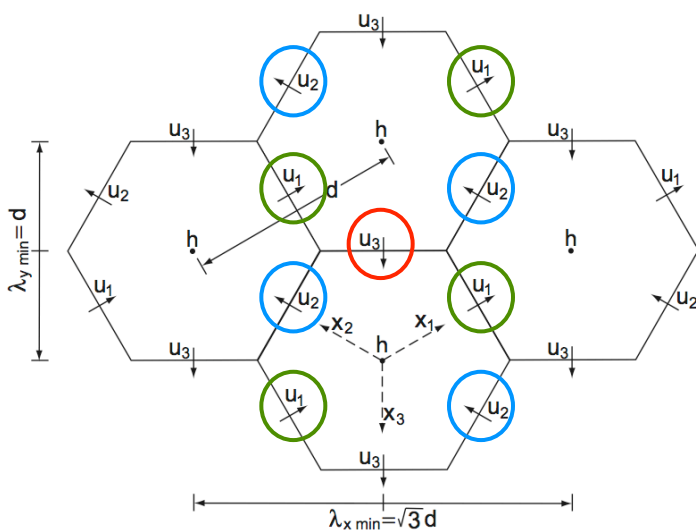
Linear piece: $f \ k \ x \ V_H$

$$\partial_t u_1 + g\delta_{x_1} h + \frac{f}{\sqrt{3}}(u_{31} - u_{21}) = 0$$

$$\partial_t u_2 + g\delta_{x_2} h + \frac{f}{\sqrt{3}}(u_{12} - u_{32}) = 0$$

$$\partial_t u_3 + g\delta_{x_3} h + \frac{f}{\sqrt{3}}(u_{23} + u_{13}) = 0$$

$$\partial_t h + \frac{2}{3}H(\delta_{x_1} u_1 + \delta_{x_2} u_2 + \delta_{x_3} u_3) = 0$$

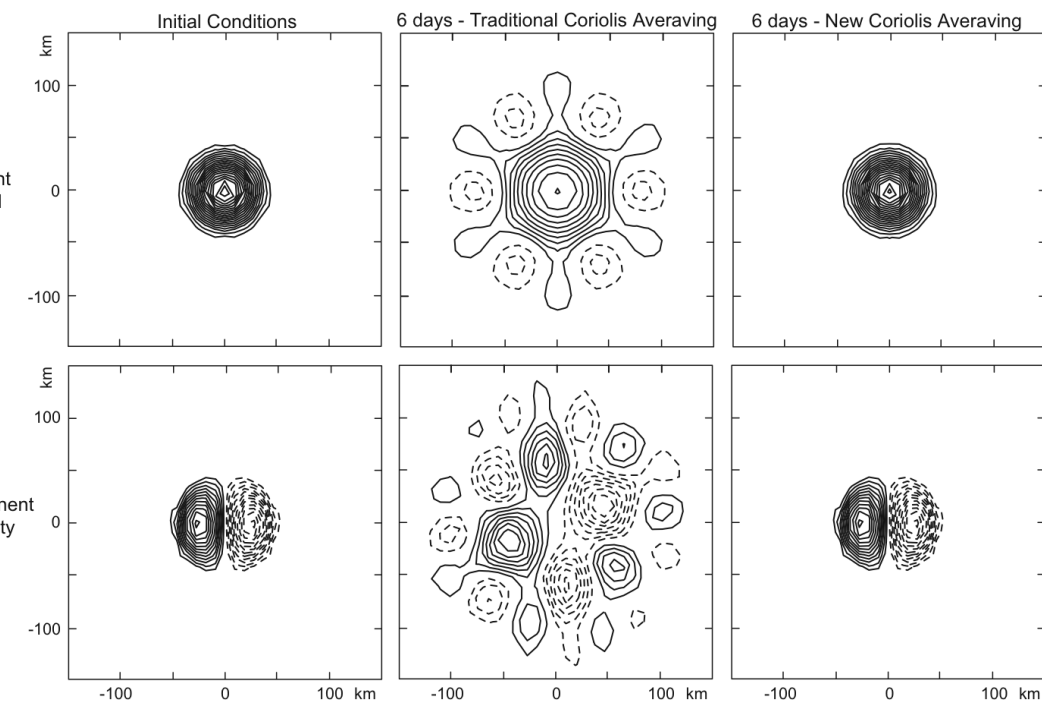


(Thuburn et al, 2009 JCP)

$$u_{21} = \frac{1}{3} \overline{u_2}^{x_3} + \frac{2}{3} \overline{\overline{u_2}}^{x_1 x_2}, \quad u_{31} = \frac{1}{3} \overline{u_3}^{x_2} + \frac{2}{3} \overline{\overline{u_3}}^{x_1 x_3},$$

$$u_{12} = \frac{1}{3} \overline{u_1}^{x_3} + \frac{2}{3} \overline{\overline{u_1}}^{x_1 x_2}, \quad u_{32} = \frac{1}{3} \overline{u_3}^{x_1} + \frac{2}{3} \overline{\overline{u_3}}^{x_2 x_3},$$

$$u_{13} = \frac{1}{3} \overline{u_1}^{x_2} + \frac{2}{3} \overline{\overline{u_1}}^{x_1 x_3}, \quad u_{23} = \frac{1}{3} \overline{u_2}^{x_1} + \frac{2}{3} \overline{\overline{u_2}}^{x_2 x_3}$$



Operators on the Voronoi Mesh

'Nonlinear' Coriolis force

Why does this work?

In the discrete analogue of vorticity equation ($\xi_t = -f \delta_a$), the divergence δ_a on the Delaunay triangulation is identical to the divergence δ_A on the Voronoi hexagons used in the height equation ($h_t = -H \delta_A$) integrated over the triangle.

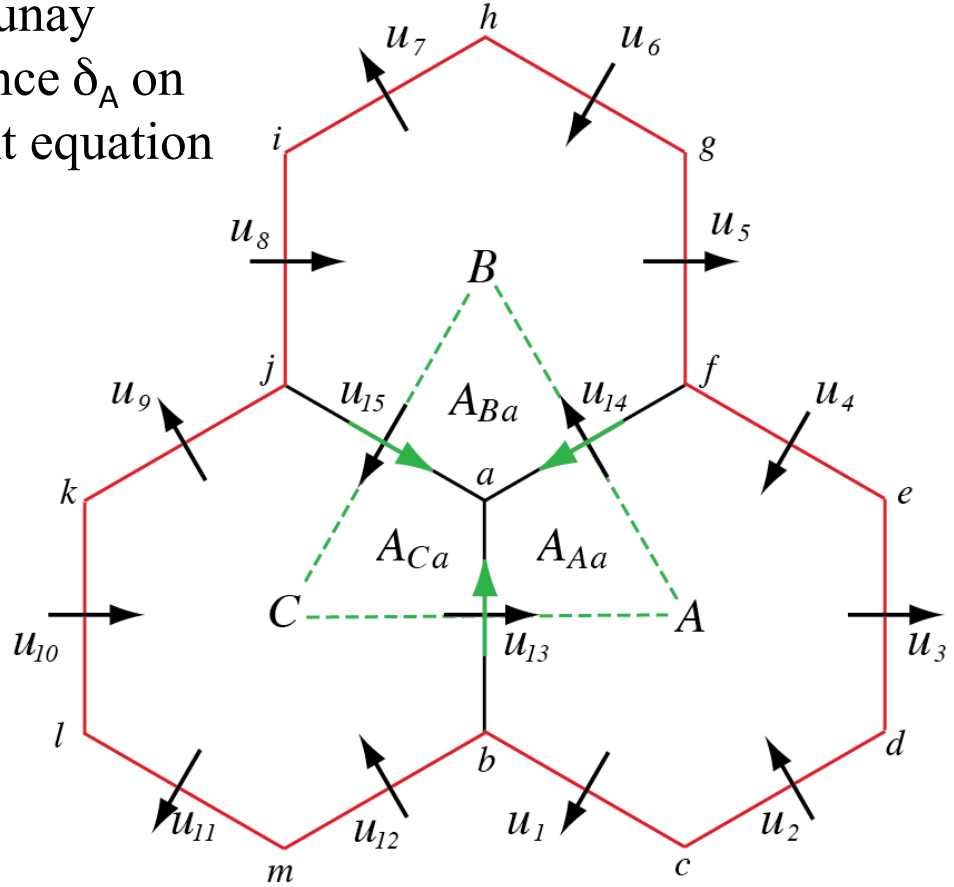
$$A_a \delta_a = \frac{A_A \delta_A + A_B \delta_B + A_C \delta_C}{6}$$

Divergence δ_A in hexagon A:

$$A_A \delta_A = \sum_{i=1}^6 l_i u_i \cdot \mathbf{n}_i$$

Divergence δ_a in triangle ABC:

$$A_a \xi_t = -f A_a \delta_a = f \sum_{j=1}^3 d_j u_j^\perp \cdot \mathbf{n}_j$$



Operators on the Voronoi Mesh

'Nonlinear' Coriolis force

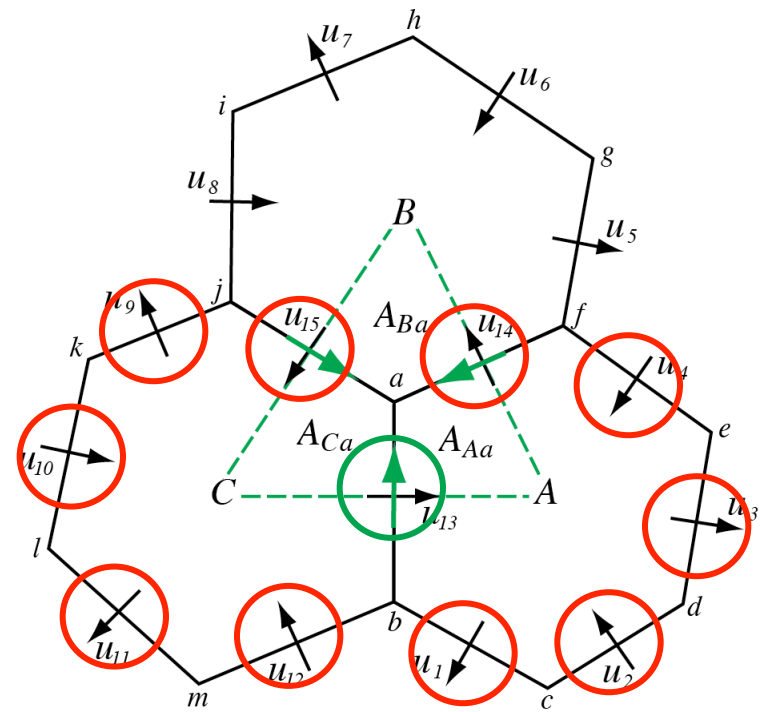
Linear piece: $f \ k x V_H$

Generalization for the Voronoi mesh:

Construct tangential velocities from weighted sum of normal velocities on edges of adjacent hexagons.

$$d_e u_e^\perp = \sum_j w_e^j l_j u_j$$

Result: geostrophic modes are stationary; local and global mass and PV conservation is satisfied on the dual (triangular) mesh (for the SW equations).



Operators on the Voronoi Mesh 'Nonlinear' Coriolis force

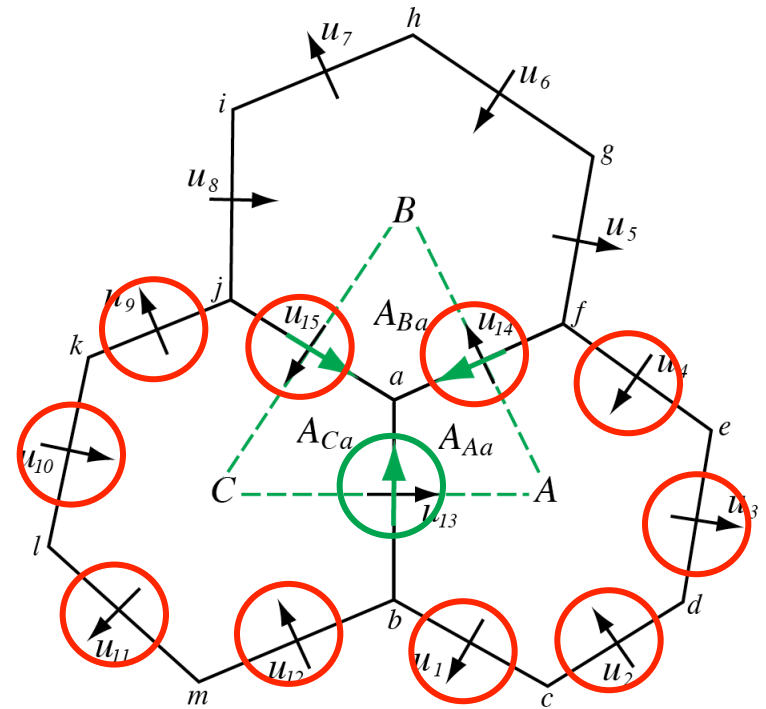
$$\begin{aligned} \frac{\partial \mathbf{V}_H}{\partial t} = & -\frac{\rho_d}{\rho_m} \left[\nabla_\zeta \left(\frac{p}{\zeta_z} \right) - \frac{\partial \mathbf{z}_H p}{\partial \zeta} \right] - \eta \mathbf{k} \times \mathbf{V}_H \\ & - \mathbf{v}_H \nabla_\zeta \cdot \mathbf{V} - \frac{\partial \Omega \mathbf{v}_H}{\partial \zeta} - \rho_d \nabla_\zeta K - eW \cos \alpha_r - \frac{uW}{r_e} + \mathbf{F}_{V_H}, \end{aligned}$$

Nonlinear term:

$$v_{e_i} = \sum_{j=1}^{n_{e_i}} w_{e_{i,j}} u_{e_{i,j}}$$

$$[\eta \mathbf{k} \times \mathbf{V}_H]_{e_i} = \sum_{j=1}^{n_{e_i}} \frac{1}{2} (\eta_{e_i} + \eta_{e_{i,j}}) w_{e_{i,j}} \rho_{e_{i,j}} u_{e_{i,j}}$$

The general tangential velocity reconstruction produces a consistent divergence on the primal and dual grids, and allows for PV, enstrophy and energy* conservation in the nonlinear SW solver.





Configuring the dynamics and the physics

(namelist.atmosphere)

```
&nhyd_model
  config_dt = 75
  config_start_time = "0000-01-01_00:00:00"
  config_run_duration = "20_00:00:00"
  config_number_of_sub_steps = 6
  config_h_mom_eddy_visc2 = 0
  config_h_mom_eddy_visc4 = 0
  config_v_mom_eddy_visc2 = 0
  config_h_theta_eddy_visc2 = 0
  config_h_theta_eddy_visc4 = 0
  config_v_theta_eddy_visc2 = 0
  config_horiz_mixing = "2d_smagorinsky"
  config_len_disp = 15000.
  config_visc4_2dsmag = 0.05
  config_h_ScaleWithMesh = .true.
  config_w_adv_order = 3
  config_theta_adv_order = 3
  config_scalar_adv_order = 3
  config_u_vadv_order = 3
  config_w_vadv_order = 3
  config_theta_vadv_order = 3
  config_scalar_vadv_order = 3
  config_positive_definite = .false.
  config_monotonic = .true.
  config_coef_3rd_order = 0.25
  config_epssm = 0.1
  config_smdiv = 0.1
```

Configuring the dynamics and the physics

(*namelist.atmosphere*)

```
&nhyd_model
  config_dt = 75
  config_start_time = "0000-01-01_00:00:00"
  config_run_duration = "20_00:00:00"
  config_number_of_sub_steps = 6
  config_h_mom_eddy_visc2 = 0
  config_h_mom_eddy_visc4 = 0
  config_v_mom_eddy_visc2 = 0
  config_h_theta_eddy_visc2 = 0
  config_h_theta_eddy_visc4 = 0
  config_v_theta_eddy_visc2 = 0
  config_horiz_mixing = "2d_smagorinsky"
  config_len_disp = 15000.
  config_visc4_2dsmag = 0.05
  config_h_ScaleWithMesh = .true.
  config_w_adv_order = 3
  config_theta_adv_order = 3
  config_scalar_adv_order = 3
  config_u_vadv_order = 3
  config_w_vadv_order = 3
  config_theta_vadv_order = 3
  config_scalar_vadv_order = 3
  config_positive_definite = .false.
  config_monotonic = .true.
  config_coef_3rd_order = 0.25
  config_epssm = 0.1
  config_smdiv = 0.1
```

Time and time-steps

&nhyd_model

```
  config_dt = 75 ← Timestep in seconds
  config_start_time = "0000-01-01_00:00:00"
  config_run_duration = "20_00:00:00"
  config_number_of_sub_steps = 6 ← Number of acoustic steps per timestep
```

(namelist.atmosphere)

```
&nhyd_model
  config_dt = 75
  config_start_time = "0000-01-01_00:00:00"
  config_run_duration = "20_00:00:00"
  config_number_of_sub_steps = 6
  config_h_mom_eddy_visc2 = 0
  config_h_mom_eddy_visc4 = 0
  config_v_mom_eddy_visc2 = 0
  config_h_theta_eddy_visc2 = 0
  config_h_theta_eddy_visc4 = 0
  config_v_theta_eddy_visc2 = 0
  config_horiz_mixing = "2d_smagorinsky"
  config_len_disp = 15000.
  config_visc4_2dsmag = 0.05
  config_h_ScaleWithMesh = .true.
  config_w_adv_order = 3
  config_theta_adv_order = 3
  config_scalar_adv_order = 3
  config_u_vadv_order = 3
  config_w_vadv_order = 3
  config_theta_vadv_order = 3
  config_scalar_vadv_order = 3
  config_positive_definite = .false.
  config_monotonic = .true.
  config_coef_3rd_order = 0.25
  config_epssm = 0.1
  config_smdiv = 0.1
```

Configuring the dynamics and the physics

Dissipation

&nhyd_model

```
config_h_mom_eddy_visc2 = 0 ← fixed viscosity m2s-1
config_h_mom_eddy_visc4 = 0 ← Fixed hyper-viscosity m4s-1
config_v_mom_eddy_visc2 = 0
config_h_theta_eddy_visc2 = 0
config_h_theta_eddy_visc4 = 0
config_v_theta_eddy_visc2 = 0
config_horiz_mixing = "2d_smagorinsky" ← Alternately "2d_fixed"
config_len_disp = 15000. ← Δx_fine
config_visc4_2dsmag = 0.05 ←
config_h_ScaleWithMesh = .true.
```

*Scale viscosities, hyperviscosities
with local mesh spacing*

*4th order background
filter coef, used with
2d_smagorinsky*

(namelist.atmosphere)

```
&nhyd_model
  config_dt = 75
  config_start_time = "0000-01-01_00:00:00"
  config_run_duration = "20_00:00:00"
  config_number_of_sub_steps = 6
  config_h_mom_eddy_visc2 = 0
  config_h_mom_eddy_visc4 = 0
  config_v_mom_eddy_visc2 = 0
  config_h_theta_eddy_visc2 = 0
  config_h_theta_eddy_visc4 = 0
  config_v_theta_eddy_visc2 = 0
  config_horiz_mixing = "2d_smagorinsky"
  config_len_disp = 15000.
  config_visc4_2dsmag = 0.05
  config_h_ScaleWithMesh = .true.
  config_w_adv_order = 3
  config_theta_adv_order = 3
  config_scalar_adv_order = 3
  config_u_vadv_order = 3
  config_w_vadv_order = 3
  config_theta_vadv_order = 3
  config_scalar_vadv_order = 3
  config_positive_definite = .false.
  config_monotonic = .true.
  config_coef_3rd_order = 0.25
  config_epssm = 0.1
  config_smdiv = 0.1
```

Configuring the dynamics and the physics

Advection

&nhyd_model

```
  config_w_adv_order = 3
  config_theta_adv_order = 3
  config_scalar_adv_order = 3
  config_u_vadv_order = 3
  config_w_vadv_order = 3
  config_theta_vadv_order = 3
  config_scalar_vadv_order = 3
  config_positive_definite = .false.
  config_monotonic = .true.
  config_coef_3rd_order = 0.25
```

Advection scheme order (2, 3, or 4)

PD/Mono options for scalar transport

*Upwind coefficient (0 <-> 1),
>0 increases damping*

(*namelist.atmosphere*)

Configuring the dynamics and the physics

Other dynamics...

&nhyd_model

...

config_epssm = 0.1 ← *off-centering of vertically implicit integration*

config_smdiv = 0.1 ← *3D divergence damping*

/

&damping

config_zd = 37000. ← *height to begin gravity wave absorbing layer (m)*

config_xnutr = 0.2 ← *gravity-wave absorbing layer coefficient*

(namelist.atmosphere)

```
&physics
  config_frac_seaice      = .false.
  config_sfc_albedo        = .true.
  config_sfc_snowalbedo    = .true.
  config_sst_update        = .false.
  config_sstdiurn_update   = .false.
  config_deepsoiltemp_update = .false.
  config_o3climatology    = .true.
  config_bucket_update     = 'none'
  config_bucket_rainc     = 100.0
  config_bucket_rainnc    = 100.0
  config_bucket_radt      = 1.0e9
  config_radtlw_interval  = '00:30:00'
  config_radtsw_interval  = '00:30:00'
  config_conv_interval     = 'none'
  config_pbl_interval      = 'none'
  config_n_microp          = 1
  config_microp_scheme     = 'wsm6'
  config_conv_deep_scheme  = 'tiedtke'
  config_lsm_scheme        = 'noah'
  config_pbl_scheme        = 'ysu'
  config_gwdo_scheme       = 'off'
  config_radt_cld_scheme   = 'cld_fraction'
  config_radt_lw_scheme    = 'rrtmg_lw'
  config_radt_sw_scheme    = 'rrtmg_sw'
  config_sfclayer_scheme   = 'monin_obukhov'
```

Configuring the dynamics and the physics

Physics schemes

config_microp_scheme	= 'wsm6' <i>(kessler, off)</i>
config_conv_deep_scheme	= 'tiedtke' <i>(kain_fritsch, off)</i>
config_lsm_scheme	= 'noah' <i>(off)</i>
config_pbl_scheme	= 'ysu' <i>(off)</i>
config_gwdo_scheme	= 'off' <i>(ysu_gwdo)</i>
config_radt_cld_scheme	= 'cld_fraction' <i>(off, cld_incidence)</i>
config_radt_lw_scheme	= 'rrtmg_lw' <i>(off, cam_lw)</i>
config_radt_sw_scheme	= 'rrtmg_sw' <i>(off, cam_sw)</i>
config_sfclayer_scheme	= 'monin_obukhov' <i>(off)</i>



MPAS Atmosphere Public Releases

[MPAS Home](#)

Overview

[MPAS-Atmosphere](#)

[MPAS-Land Ice](#)

[MPAS-Ocean](#)

[Data Assimilation](#)

[Publications](#)

[Presentations](#)

Download

[MPAS-Atmosphere download](#)

[MPAS-Land ice download](#)

[MPAS-Ocean download](#)

Resources

[License Information](#)

[Wiki](#)

[Bug Tracker](#)

[Mailing Lists](#)

[MPAS Developers Guide](#)

MPAS Atmosphere 2.1 was released on 6 June 2014.

Any questions related to building and running MPAS-Atmosphere should be directed to the [MPAS-Atmosphere Help](#) forum. Posting to the forum requires a free google account. Alternatively, questions may be sent from any e-mail address to "mpas-atmosphere-help AT googlegroups.com". Please note that in either case, questions and their answers will appear on the online forum.

[MPAS Atmosphere 2.1 release notes](#)

[MPAS source code download](#)

[MPAS Atmosphere Users Guide](#)

[MPAS Atmosphere meshes](#)

[Configurations for idealized test cases](#)

[Sample input files for real-data simulations](#)

[Visualization and analysis tools](#)



A variable resolution MPAS Voronoi mesh

MPAS Solver Information

<http://mpas-dev.github.io/>



[MPAS Home](#)

Overview

[MPAS-Atmosphere](#)

[MPAS-Land Ice](#)

[MPAS-Ocean](#)

[Data Assimilation](#)

[Publications](#)

[Presentations](#)

Download

[MPAS-Atmosphere download](#)

[MPAS-Land Ice download](#)

[MPAS-Ocean download](#)

Resources

[License Information](#)

[Wiki](#)

[Bug Tracker](#)

[Mailing Lists](#)

[MPAS Developers Guide](#)

Peer-reviewed publications relevant to MPAS

2013

Evaluation of global atmospheric solvers using extensions of the Jablonowski and Williamson baroclinic wave test case. S.-H. Park, W. Skamarock, J. Klemp, L. Fowler, and M. Duda, 2013, accepted for publication in Monthly Weather Review, [pdf](#)

A Multiresolution Approach to Global Ocean Modeling. T. Ringler, M. Petersen, R.L. Higdon, D.W. Jacobsen, P.W. Jones and M. Maltrud, 2012: , Ocean Modeling, revised ([pdf](#)).

2012

Exploring a Global Multi-Resolution Modeling Approach Using Aquaplanet Simulations. S. Rauscher, T. Ringler, W. Skamarock, and A. Mirin, 2012, in press, Journal of Climate, [pdf](#)

A Multi-scale Nonhydrostatic Atmospheric Model Using Centroidal Voronoi Tesselations and C-Grid Staggering. William C. Skamarock, Joseph B. Klemp, Michael G. Duda, Laura Fowler, Sang-Hun Park, and Todd D. Ringler. 2012 Monthly Weather Review, 240, 3090-3105, doi:10.1175/MWR-D-11-00215.1 [pdf](#)



2011

A Terrain-Following Coordinate with Smoothed Coordinate Surfaces. Joseph B. Klemp, 2011, Monthly Weather Review, 139(7), 2163–2169. [doi:10.1175/MWR-D-10-05046.1](#)

Conservative Transport Schemes for Spherical Geodesic Grids: High-Order Flux Operators for ODE-Based Time Integration. W. Skamarock and A. Gassmann, 2011, Monthly Weather Review, Vol. 139, pp. 2962-2975, doi:10.1175/MWR-D-10-05056.1 [pdf](#)